Check for
updates

Probing semiconductor quantum well qubits and associated Shannon entropy using semi-relativistic quantum mechanics

Moletlanyi Tshipa[1]

Abstract

Electron states in *GaAs*, *GaN* and *AlN* quantum wells are studied by solving a semi-relativistic wave equation within the effective mass approximation. The quantum states are in turn used to probe the properties of two-level qubits formed in the different quantum wells at various temperatures. Results indicated that the period of oscillation between the quantum states increases with increasing width of the quantum wells, with *AlN* having the longest period and shortest for *GaAs*. Transition rates were also studied, since their product with the period of oscillation yield important information concerning the feasibility of carrying out a quantum computation. This product is equivalent to the ratio of the period of oscillation between states to the lifetime of an electron in an excited state. From the results, *GaAs* quantum wells may be preferable as they have the lowest ratio compared with the other quantum wells of other materials. *AlN* has the highest ratio of the three semiconductors considered here. Shannon entropy in the different quantum wells was studied also. It was found that the entropy in *GaAs* quantum wells varies rapidly through the passage of time, while those of *GaN* and *AlN* vary relatively slowly.

Keywords Semi-relativistic quantum mechanics · Quantum well · Qubits

1 Introduction

Nanotechnology, the ability to have control over the architecture of devices at a nanoscale, has been quite instrumental in realizing a plethora of quantum structures (Xia et al. 2003; Liang et al. 2019; Wu et al. 2021; Li et al. 2021). These quantum structures are crucial since they confine charge carriers to regions in the nanometer scale, giving rise to quantum effects. It is from these quantum effects that many applications spring forth, for example in laser technology (Marko et al. 2016), optoelectronics (Ghetmiri et al. 2017), food technology (Pathakoti et al. 2017), energy storage (Reddy et al. 2012), and so forth. The immense potential of quantum structures has fueled a lot of research on these structures. Linear and nonlinear optical properties of quantum dots have been reported on (Chang et al. 2023). It

✉ Moletlanyi Tshipa
  tshipam@ub.ac.bw

[1] Department of Physics, University of Botswana, Corner of Notwane and Mobuto Road, Gaborone, Botswana

has also been established that quantum structures can facilitate second and third harmonic generation of electromagnetic radiation (Tshipa 2021; Chang 2023). Among these nanostructures are quantum wells (QWs) (Pan et al. 2012; Wang et al. 2018; Sammak et al. 2019), which are relatively easier and cheaper to fabricate. As such, there has been some interest in investigating properties of quantum wells (Knez et al. 2011; Chrafih et al. 2019; Henning et al. 2021; Zhang et al. 2011, 2019).

One of the recent fields of application of nanostructures has been in the field of quantum computing. Consequently, there has been a lot of both theoretical and experimental research into quantum computing. Due to quantization effects, information can be encoded and manipulated in quantum structures. Existence and persistence of qubits in these structures are the cornerstones of quantum computing. It is, thus, crucial to shield computational space from interaction with the surrounding media, hence the effect of the environment, in the form of "quantum noise", has been explored by Berrada et al (Berrada and Aldaghri 2019) while implications of the interaction of a qubit with parity deformed field have been reported on (Abdel-Khalek et al. 2023). As a way of fabricating nanostructures optimized for quantum computing, McJunkin et al proposed and fabricated a *SiGe* quantum well with undulating *Ge* concentration (McJunkin et al. 2022).

Another challenge is obtaining long coherence times. Quantum computations can only proceed as long as qubits persist. Thus, the time it takes for a qubit to decohere, coherence time, has been studied extensively. Feng et al. theoretically explored the effect of a homogeneous magnetic field on coherence time of qubits in asymmetric Gaussian potential quantum wells, and showed that the coherence time increases with decreasing cyclotron frequency of the applied magnetic field (Feng et al. 2022). As these nanostructures may contain impurities, it is imperative to have a proper understanding of the effects of impurities on properties of qubits. Thus, effects of hydrogenic impurity on the evolution of a qubit in the presence of phonons have been studied in an asymmetric Gaussian potential quantum well (Xiao et al. 2015). It was shown that the period of oscillation of the electron probability density between the ground state and the excited states decreases with increase in the impurity potential and the polaron radius. Lately, the effect of a hydrogenic impurity on the Shannon entropy (an index of uncertainty associated with events that occur with various probabilities) of a two level qubit system in elliptical, circular and triangular quantum dots has been investigated (Khordad and Sedehi 2020). In the paper, it is shown that the geometry of the quantum dots may be used to modify coherence time.

This research is concerned with probing the properties of two level qubits formed in quantum wells using the semi-relativistic quantum mechanics. We describe the approach as semi-relativistic because this approach yields accurate values even as confinement energy increases, but not relativistic in the sense of the Dirac equation. This research is organized as follows: Sect. 2 is aimed at erecting the theoretical framework of the problem, whose results are discussed in Sect. 3 and the conclusions laid in Sect. 4.

2 Theoretical framework

2.1 Wave equations

In the spirit of Einstein (Einstein 1905), the energy of a particle (of an electron in this case) of effective mass m_0 traveling with velocity v is given by

$$E = \frac{m_0 c^2}{\sqrt{1 - \beta^2}} + V, \tag{1}$$

where $\beta = v/c$, c being the speed of light in vacuum and V is potential energy of the system. The above equation can be rewritten as

$$(E - V)^2 = \frac{m_0^2 c^4}{(1 - \beta^2)}. \tag{2}$$

Following Schrödinger, to imbue the particle with wavelike properties, we ascribe to it a wave function ψ with which Eq. (2) can be multiplied to give

$$(E - V)^2 \psi = \frac{m_0^2 c^4}{(1 - \hat{\beta}^2)} \psi, \tag{3}$$

which can be rewritten as

$$\hat{\beta}^2 \psi = \left[1 - \frac{m_0^2 c^4}{(E - V)^2} \right] \psi. \tag{4}$$

where $\hat{\beta} = \hat{p}/m_0 c$ is a quantum mechanical operator equivalent of β, where $\hat{p} = -i\hbar\nabla$. Here, $i^2 = -1$ and $\hbar = h/2\pi$, h being Planck's constant. This implies that the above equation can be cast as

$$\nabla^2 \psi + \left[\frac{m_0^2 c^2}{\hbar^2} - \frac{m_0^4 c^6}{\hbar^2 (V - E)^2} \right] \psi = 0. \tag{5}$$

which is the semi-relativistic wave equation utilized in this research.

2.2 Wave functions

As a demonstration of Eq. (5), we shall consider an electron confined in a one dimensional infinite quantum well. This system can be achieved by sandwiching a semiconductor material in a glass matrix or any other semiconductor with very large band gap, large enough to be considered infinite for practical purposes. The electric potential for this case is

$$V = V(z) = \begin{cases} 0 & 0 < z < L \\ \infty & elsewhere \end{cases}$$

where L is width of the quantum well. With the electric potential V given as above, Eq. (5) now reads

$$\nabla^2 \psi + \left[\frac{m_0^2 c^2}{\hbar^2} - \frac{m_0^4 c^6}{\hbar^2 E^2} \right] \psi = 0, \tag{6}$$

which may be written as

$$\nabla^2 \psi + \kappa^2 \psi = 0, \tag{7}$$

where

$$\kappa = \frac{m_0 c \sqrt{(E^2 - m_0^2 c^4)}}{\hbar E}. \tag{8}$$

In the direction of confinement, (Eq. 7) is solvable in terms of the sine and cosine functions

$$\chi(x) = C_1 \cos(\kappa z) + C_2 \sin(\kappa z). \tag{9}$$

The electric potential is infinite outside the quantum well, hence the wave function must vanish at the walls of the QW ($\chi(z = 0) = \chi(z = L) = 0$). Applying the boundary condition $\chi(z = 0) = 0$ we get $C_1 = 0$, that is

$$\chi(z) = C_2 \sin(\kappa z). \tag{10}$$

In order to satisfy the second boundary condition, the argument of the sine function must be integer multiple of π, that is,

$$\kappa L = n\pi, \tag{11}$$

where n in an integer, or, using Eq. (8)

$$\sqrt{\frac{m_0^2 c^2 (E^2 - m_0^2 c^4)}{\hbar^2 E^2}} L = n\pi, \tag{12}$$

Making the E the subject of formula in Eq. (12) gives

$$E = \pm \frac{m_0 c^2}{\sqrt{1 - \frac{n^2 \hbar^2 \pi^2}{m_0^2 c^2 L^2}}}, \tag{13}$$

reminiscent of higher order Schrödinger equations energy eigen values (Carles and Moulay 2012). Thus, for motion of the electron unimpeded in two directions with the total wave function

$$\psi(x, y, z) = C_n \sin(\kappa z) exp[i(k_x x + k_y y)], \tag{14}$$

the total energy is expressible as

$$E = \pm \frac{m_0 c^2}{\sqrt{1 - \frac{n^2 \hbar^2 \pi^2}{m_0^2 c^2 L^2}}} + \frac{\hbar^2 (k_x^2 + k_y^2)}{2m_0}, \tag{15}$$

where k_x and k_y are the electron's wave numbers in the x and y directions respectively.

2.3 Temperature dependence of quantum well parameters

The temperature dependence of electron effective mass for the *GaAs* is specified by (E Iqraoun et al. 2021)

$$m_0 = m_0(T) = m_e \left[1 + E_g^\Gamma \left(\frac{2}{E_g(T)} + \frac{1}{E_g(T) + \Delta_0} \right) \right]^{-1}, \tag{16}$$

where m_e is mass of the free electron, E_g^Γ is the energy gap between the valence band and the conduction band at the Γ valley in a semiconductor and Δ_0 is the spin-orbit splitting. For *GaN* and *AlN*, the empirical formal (Belaid et al. 2022)

$$m_0 = m_0(T) = m_e \left[1 + \frac{C}{E_g(T)} \right]^{-1}, \tag{17}$$

has been used, where C is the energy associated with the momentum matrix element, whose value is given in Table 1. The temperature dependence of the band-gap $E_g(T)$ is given by the empirical Varshni formula (Belaid et al. 2022)

$$E_g(T) = E(0) - \frac{\alpha T^2}{T + \beta}. \tag{18}$$

Here, $E(0)$ is the value of the band gap at $T = 0$, and α and β are parameters with values unique to a specific semiconductor, given in Table 1.

Temperature dependence of the dielectric constant for *GaAs* has been taken as (E Iqraoun et al. 2021)

$$\epsilon_{m(GaAs)}(T) = \left\{ \begin{array}{ll} 12.7 \exp[(9.4 \times 10^{-5})(T - 75.6)], & \text{for } 0 < T < 200K \\ 13.18 \exp[(20.4 \times 10^{-5})(T - 300)], & \text{for } T > 200K \end{array} \right\}, \tag{19}$$

for *AlN* and *GaN*, respectively (Belaid et al. 2022)

$$\epsilon_{m(AlN)}(T) = 8.5 \exp(10^{-4}(T - 300)), \tag{20}$$

$$\epsilon_{m(GaN)}(T) = 9.5 \exp(10^{-4}(T - 300)). \tag{21}$$

2.4 Qubits

Here, we study a two-level qubit consisting of a superposition of the ground state $|i\rangle$ and the excited state $|f\rangle$. The superposition is expressed mathematically as

$$|\psi_{if}\rangle = (|i\rangle + |f\rangle)/\sqrt{2}. \tag{22}$$

Using the time evolution of the electron quantum state in the 2 level system

Table 1 Physical parameters of *GaAs*, *GaN* and *AlN* used in these computations

Semi- conductor	Δ_0 (meV)	E_g^Γ (meV)	E(0) (meV)	α (meV/K)	β (K)	C (meV)
GaAs	341[1]	7510[1]	1519[1]	0.5405[1]	204[1]	–
GaN	–	–	3299[2]	0.909[2]	830[2]	14670[2]
AlN	–	–	6230[2]	1.799[2]	1462[2]	17910[2]

[1](E Iqraoun et al. 2021)

[2] (Belaid et al. 2022)

$$\psi_{if}(\mathbf{x}, t) = \frac{1}{\sqrt{2}}\left[\psi_i(\mathbf{x})\exp\left(-\frac{iE_it}{\hbar}\right) + \psi_f(\mathbf{x})\exp\left(-\frac{iE_ft}{\hbar}\right)\right], \qquad (23)$$

the probability density of the electron can be expressed as

$$
\begin{aligned}
D_{if}(\mathbf{x}, t) &= |\psi_{if}(\mathbf{x}, t)|^2 \\
&= \frac{1}{2}\left[|\psi_i(\mathbf{x})|^2 + |\psi_f(\mathbf{x})|^2 + \psi_i^*(\mathbf{x})\psi_f(\mathbf{x})\exp(i\omega_{if}t) + \psi_i(\mathbf{x})\psi_f^*(\mathbf{x})\exp(-i\omega_{if}t)\right]
\end{aligned}
$$
$$(24)$$

where the asterisk signifies complex conjugate and $\omega_{if} = (E_f - E_i)/\hbar$ is the angular frequency associated with transition between the ground state and the first excited state. The period of oscillation of the probability density of the electron between an initial state with energy E_i and a final state with energy E_f can be expressed as

$$T_0 = \frac{h}{(E_f - E_i)}. \qquad (25)$$

2.5 Shannon entropy

Shannon entropy is a measure of the randomness or uncertainty in a random variable, which is indicative of the expected value of information content within a message; that is, the number of qubits required to encode and transmit the message without loss of information. Its applications are wide ranged: microseismic detection (da Silva and Corso 2022), biomedical signal analysis (Vakkuri et al. 2004) and econometric/financial time series analysis (Golan and Maasoumi 2008), to cite a few. In quantum information theory, it is indicative of the localization information of the probability distribution, which gives good description of quantum systems (Shi et al. 2017; Edet and Ikot 2021). It can also reflect the complexity of a time series: low entropy indicating low complexity (less randomness or more structure) and vice versa (Nagaraj and Balasubramanian 2017). Shannon entropy is evaluated according to (Khordad and Sedehi 2020)

$$S = \int \psi_{if}(\mathbf{x}, t)^2 ln(\psi_{if}(x, t)^2)d\tau \qquad (26)$$

where $d\tau$ is the elemental volume corresponding to a particular coordinate system. Here, we have neglected the effects of the external environment which may affect quantum computations, which have been dealt with elsewhere (Nagaraj and Balasubramanian 2017; Li 2018; da Silva and Corso 2022; Han et al. 2022). For example, provided that signal-to-noise ratio is not too low, noisy channels may turn out to be more suitable for a cleaner communication due to interference from the noisy processes (Chiribella1 and Kristjánsson 2019).

2.6 Transition rates

We consider an electromagnetic (EM) radiation incident on an electron confined in a QW. The electron in an initial state of energy E_i can absorb energy from the EM radiation and transition to a final state of energy E_f, provided the energy of the EM radiation

equals the energy difference between the states, $\Delta E = E_f - E_i$. The rate at which this transition happens can be calculated using the Fermi Golden rule (Atić et al. 2022)

$$W_{fi} = \frac{2\pi}{\hbar} |\langle \psi_f | H_{int} | \psi_i \rangle|^2 \delta(E_f - E_i \pm \hbar\omega), \tag{27}$$

where the electron-photon interaction H_{int} is given by

$$H_{int} = -\frac{e}{\mu} \vec{A}_\omega \cdot \vec{p} = -\frac{e}{2\mu} A_0 [e^{i(\vec{q}\cdot\vec{r}-\omega t)} + e^{-i(\vec{q}\cdot\vec{r}-\omega t)}] \hat{\epsilon} \cdot \vec{p}. \tag{28}$$

Here, $\vec{q}$ the photon field wave vector, $\vec{r}$ the electron position vector, $\hat{\epsilon}$ is the unitary polarization vector of the radiation field and A_0 is the amplitude of the vector potential. The amplitude of the vector potential can be written as $A_0 = \sqrt{(N_q\hbar)/(2\epsilon_0\epsilon_w\omega V)}$, where N_q is the number of photons in volume V of the quantum well of dielectric constant ϵ_w and ϵ_0 is the permittivity of free space. For light linearly polarized in the z direction incident on the quantum well in the x direction, $\vec{q} = (q_x, 0, 0)$ and $\hat{\epsilon} \cdot \vec{r} = z$, thus, transition rates in a quantum well can be evaluated as

$$W_{fi} = N_q \pi e^2 (E_f - E_i)^2 / (4\epsilon_0\epsilon_w\hbar^2\omega)\langle z \rangle^2 \delta(E_f - E_i \pm \hbar\omega), \tag{29}$$

where

$$\begin{aligned}
\langle z \rangle &= \int \psi_n'(x, y, z) z \exp(iq_x x) \psi_n(x, y, z) dV \\
&= \frac{4in'nL[1 - \exp(iq_x L_x)]}{\hbar(\Delta k_x + q_x)L_x\pi^2(2n + \Delta n)^2(\Delta n)^2},
\end{aligned} \tag{30}$$

for odd Δn, where $\Delta k_x = k_x - k_x'$, and vanishes for even Δn, where $\Delta n = n' - n$. This gives the selection rules for transitions in this system. In the above, $dV = dxdydz$ is the elemental volume and the identity: $p = [\mu(E_f - E_i)r]/(i\hbar)$, in the Heisenberg equations of motion for operators (Scully and Zubairy 1997), has been used to substitute out the momentum operator in Eq. (28). Thus, for an electron wave function of the form given in Eq. (10), absorption and emission transition rates are found to be, respectively,

$$W_{fi}^{abs} = W_0 |\langle z \rangle|^2 \delta(E_f - E_i - \hbar\omega) \tag{31}$$

and

$$W_{fi}^{em} = W_0 |\langle z \rangle|^2 \delta(E_f - E_i + \hbar\omega), \tag{32}$$

where $W_0 = N_q e^2 (E_f - E_i)^2 L_x / (4\epsilon_0\epsilon_w\hbar^2\omega)$. Finally, it is helpful especially for purposes of computation, to replace the Dirac delta function with a Lorentzian factor according to

$$\delta(E_f - E_i \pm \hbar\omega) \rightarrow \frac{\gamma}{\pi(E_f - E_i \pm \hbar\omega)^2 + \gamma^2},$$

in which γ is the linewidth of resonance. The total transition rate of the quantum system involves a summation of all the individual transition rates taking into account the transition probabilities of all the allowed transitions according to (Renk 2012)

$$\Gamma_{fi}^{abs/em} = \sum W_{fi}^{abs/em} f_i (1 - f_f) \tag{33}$$

where f_i and f_f are the Fermi-Dirac distribution functions for the initial and final states respectively.

3 Results and discussions

This section is dedicated to the discussions of the theoretical calculations based on the derivations in the previous section. In these computations, $\gamma = 3.3\ meV$ has been used as the linewidth of the Dirac delta function (Aghoutane et al. 2019; Aydin et al. 2021; En-nadir et al. 2021) and $N_q = 10^{24} m^{-3}$. The wave vector of the incident photons has been taken such that $q_x L_x = 1$ and $\Delta k_x \approx 0$, that is, $k'_x \approx k_x$. The dependence of the period of oscillation T_0 on widths of $GaAs$, GaN, and AlN quantum wells can be viewed in Fig. 1. In the figure, the solid plots are for $T = 77\ K$ while the dashed plots with dots are for room temperature ($T = 300\ K$). As can be seen also in Eq. (25), the period of oscillation between states is inversely proportional to transition energies (difference in energies of states between which transitions occur). Transition energies decrease with increase in width of confinement, with transition energies corresponding to $GaAs$ being generally higher than those of GaN and AlN, those of AlN being the lowest of the three QWs considered here. Consequently, the period of oscillation has an almost parabolic increase in its variation of width of the quantum wells, that corresponding to $GaAs$ being the least of the three, and that corresponding to AlN being the longest. In quantum computing, it is desirable for the period of oscillation to be as short as possible to allow as many quantum processes to occur before decoherence of the qubit. This shows that $GaAs$ quantum wells can be more suited for qubit manipulation than those of GaN and AlN. Additionally, temperature enhances transition energies, hence increase in temperature decreases the period of oscillation. It is clear from the figure that temperature change has an appreciable effect on the period of oscillation of $GaAs$ quantum wells than those of GaN and AlN. This shows that even though the AlN quantum

Fig. 1 Period of oscillation as a function of width of $GaAs$, GaN and AlN quantum wells. The solid plots correspond to temperature of $T = 77\ K$ while the dashed plots with dots are for $T = 300\ K$
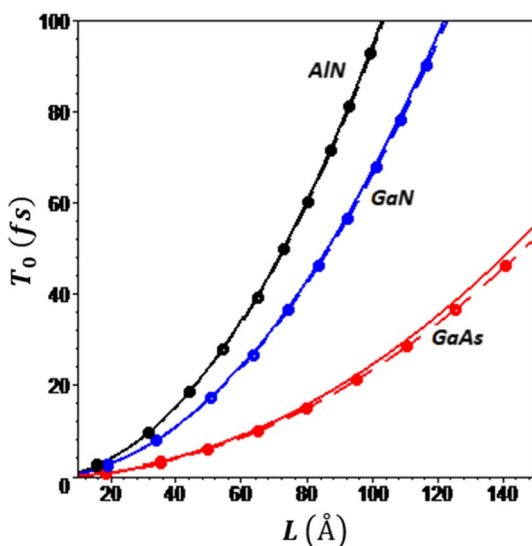
well qubits are not preferable on account of the long period of oscillation, they are the most stable against thermal fluctuations.

As already mentioned, the period of oscillation between states must be shorter than the lifetime of a particle in an excited state in order for a quantum computation to be possible. This means that quantum computations will only occur as long as superposition between the states exists, that is, before coherence is lost due to emission of some packet of energy like a photon or a phonon. As such, it becomes imperative to compare the magnitude of the period of oscillation between the states in superposition and the lifetime in an excited state. Figure 2 shows peaks of transition rates in a *GaAs* quantum well, as functions of width of the QW. The different plots have been generated for different temperatures: from 50 *K* to 550 *K* in steps of 25 *K*. The upper branch corresponds to absorption while the lower corresponds to emission. Peaks of absorption transition rates assume high values from very small widths of the QW, before decreasing asymptotically with increasing QW width. At low temperatures, peaks of absorption transition rates remain relatively constant over a considerably wider range of QW width near their maxima, before decreasing, than at high temperatures. Peaks of emission transition rates are much lower than those of absorption, and increase with increasing QW width, an increase more pronounced at high temperatures. These values are comparable to those in the literature. Citrin et al. obtained an excitonic transition lifetime of ≈ 150 *ps* for a cylindrical *GaAs* nanowire of radius $R = 100$ Å (Citrin 1993). Using Eq. (33), for a corresponding QW of width, we get a transition rate of 7.6 fs^{-1}, corresponding to lifetimes of 131.4 *ps* at room temperature (300K). Bellessa et al. performed photoluminescence measurements and extracted an excitonic lifetime of 350 *ps* for a $GaAs/Al_x Ga_{1-x} As$ quantum box of sides $L = 400$ Å at a temperature of 6 *K* (Bellessa et al. 1998). Again, with the help of Eq. (33) in conjunction with the full width at half maximum of $\gamma = 8$ *meV* stipulated in the paper, we obtain intersubband transition rates corresponding to lifetimes of 271.5 *ps*. Since quantum computations require long lifetimes τ_{fi}, which correspond to low transition rates, Fig. 2 suggests that narrower QWs would be preferable for quantum computing.

The comparison of peaks of emission and absorption transition rates for quantum wells materials, that is, *GaAs* (solid lines), *GaN* (plots with dots) and *AlN* (dashed

Fig. 2 Peaks of absorption (*Abs*) and emission (*Em*) transition rates as functions of width of a *GaAs* quantum well at the different temperatures running from 50 *K* to 550 *K* in steps of 25 *K*
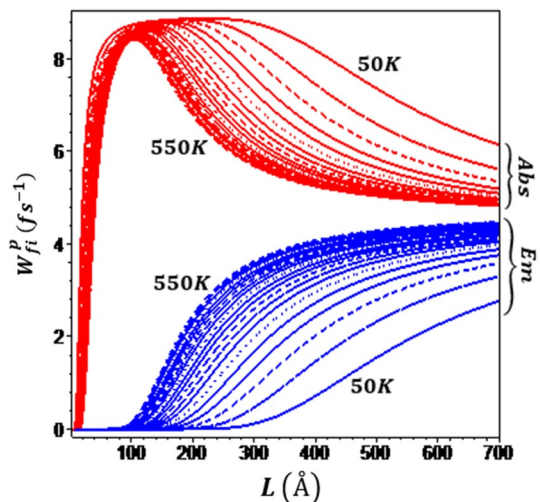
Fig. 3 Dependence of peaks of absorption (*Abs*) and emission (*Em*) transition rates on *GaAs* (solid curves), *GaN* (plots with dots) and *AlN* (dashed lines) quantum wells at 77 *K*
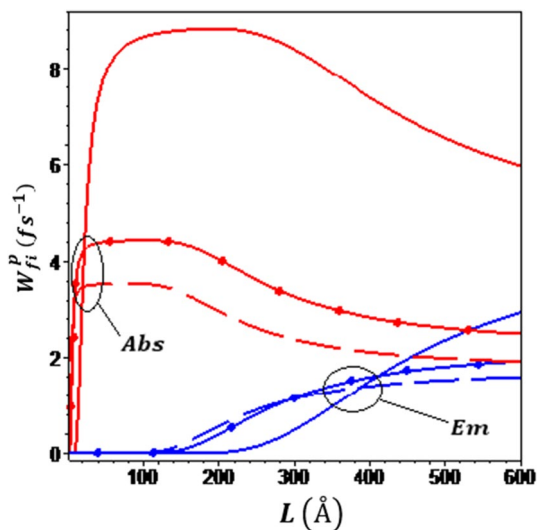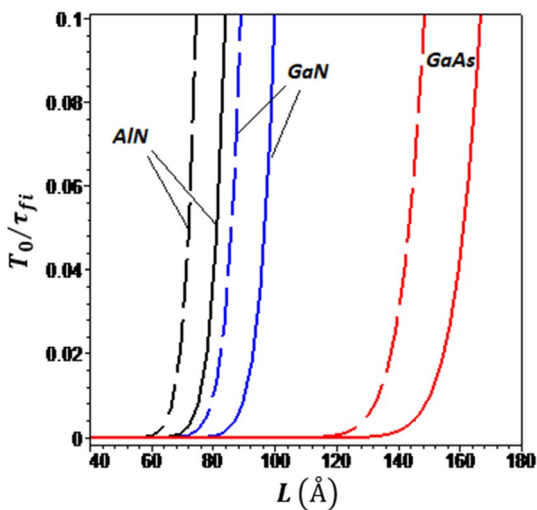

Fig. 4 Ratio of the period of oscillation between the two levels T_0 to the lifetime of a particle in the excited state τ_{fi}, corresponding to peak transition rates, as a function of width of *GaAs*, *GaN* and *AlN* quantum wells at the different temperatures: 77 *K* (solid plots) and 100 *K* (dashed curves)

curves), can be viewed in Fig. 3 for a constant temperature of 77 *K*. Absorption transition rates for *GaAs* are higher than those of *GaN* and *AlN*, with those for *GaN* being the least of the three. Emission transition rates for *GaAs* QWs are lower than those for *GaN* and *AlN* for narrow QWs, those for *AlN* being the greatest of the three. Since for quantum computations, it is desirable for emission transition rate to be as low as possible, it is clear that *GaAs* QWs are better suited to form qubits for quantum computations than *GaN* and *AlN* QWs, particularly for narrow QWs. A more representative picture is obtained from the plots of the ratio of period of oscillation (T_0) and the lifetime in an excited state (τ_{fi}). This can be viewed in Fig. 4, which depicts the dependence of the ratio (T_0/τ_{fi}) on width of *GaAs*, *GaN* and *AlN* QWs at 77 *K* (solid plots) and 100
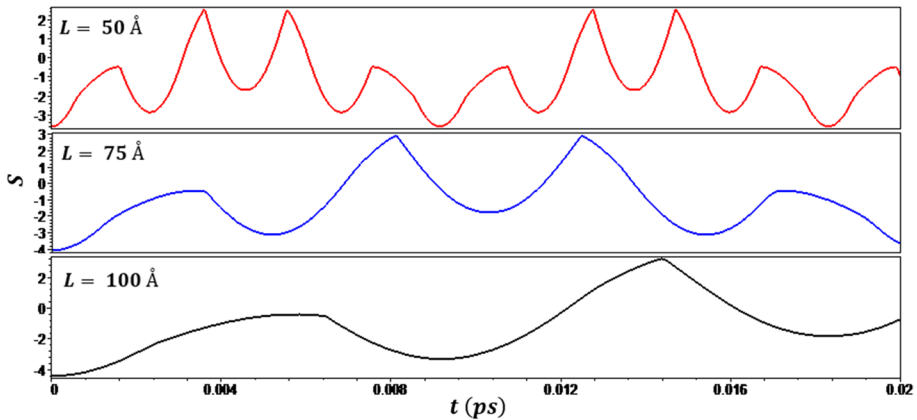
Fig. 5 Evolution of Shannon entropy of a *GaAs* quantum well qubit for three well widths: $L = 50$ Å $L = 75$ Å and $L = 100$ Å for $T = 77$ K

K (dashed curves). It is desirable that the ratio be as small as possible ($T_0/\tau_{fi} << 1$) to allow for as many quantum computational processes to occur before decoherence of the qubit. Results show that the ratio remains very low for *GaAS* QWs for a wider range of QW width than for *GaN* and *AlN* QWs. Additionally, higher temperature enhances this ratio, thus it would be advisable to run quantum computations in low temperature environments.

Figure 5 shows the evolution of Shannon entropy for a qubit in *GaAs* quantum wells of different widths: 50 Å, 75 Å and 100 Å, at 77 K. Results show that Shannon entropy of narrower quantum wells oscillates more rapidly through the passage of time than that of wider quantum wells. Thus, if it is required that the entropy should vary slowly with time in some system, then larger quantum wells would be preferable. However, due to the fact that the period of oscillation between the states is longer for wide quantum wells, it would be preferable to use narrower quantum wells as a medium for quantum computations. A consequence of using narrower quantum wells to provide computational space is that then the Shannon entropy will oscillate more rapidly with time.
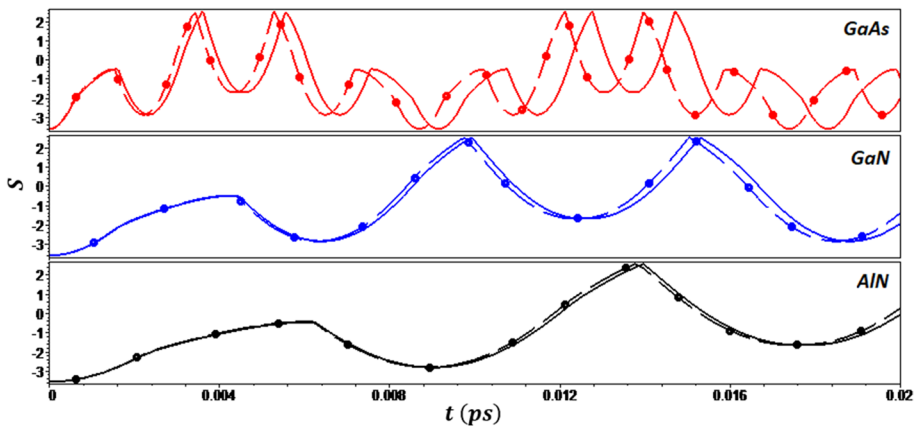

Fig. 6 Evolution of Shannon entropy of $L = 50$ Å wide *GaAs*, *GaN*, and *AlN* quantum well qubits at $T = 77$ K (solid curves) and $T = 300$ K (dashed plots with dots)

Figure 6 shows the evolution of the Shannon entropy of qubits in *GaAs*, *GaN* and *AlN* quantum wells at 77 *K* (solid plots) and at 300 *K* (dashed plots with dots). Results show that entropy of *GaAs* quantum well qubits oscillates more rapidly than those of *GaN* and *AlN* quantum wells of the same width. Thus, if a system requires entropy to vary slowly over time, then *GaN* and *AlN* QWs may be used. However, despite the fact that *GaAs* QWs experience rapid oscillation of the Shannon entropy, they are still preferable to *GaN* and *AlN* QWs as they decohere slower than both.

4 Conclusion

Shannon entropy associated with qubits formed in *GaAs*, *GaN* and *AlN* quantum wells has been investigated. This was achieved by solving a semi-relativistic wave equation within the effective mass approximation. Results indicate that Shannon entropy varies fastest in *GaAs* quantum wells, while it varies slowest in *AlN* quantum wells. Additionally, Shannon entropy of narrow quantum wells varies faster than those of wider quantum wells over time, for the quantum wells considered here. The other relevant quantities that were studied were period of oscillation of the qubit and transition rates. Of the quantum wells studied here, *GaAs* has the shortest period of oscillation, while *AlN* has the longest. Transition rates are indicative of the lifetime of an electron in an excited state. For quantum computations to be possible, this lifetime must be much greater than the period of oscillation. It turns out that *GaAs* quantum wells have the smallest ratio of period of oscillation to the lifetime, followed by *GaN* and *AlN* quantum wells respectively. Additionally, temperature raises this ratio, which implies high temperatures are detrimental to quantum computing.

Declarations

Conflict of interest The author declares no competing interests.

Ethics approval Not applicable.

Consent to participate Not applicable.

Code availability Not applicable.

References

Abdel-Khalek, S., Khalil, E.M., Alruqi, A.B., et al.: Evolution of the entanglement, photon statistics and quantum fisher information of a single qubit parity deformed jcm. Opt. Quant. Electron **55**, 161 (2023). https://doi.org/10.1007/s11082-022-04365-5

Aghoutane, N., El-Yadri, M., El Aouami, A., et al.: Excitonic nonlinear optical properties in AlN/GaN spherical core/shell quantum dots under pressure. MRS Commun. **9**, 663–669 (2019). https://doi.org/10.1557/mrc.2019.43

Atić, A., Vuković, N., Radovanović, J.: Calculation of intersubband absorption in ZnO/ZnMgO asymmetric double quantum wells. Opt. Quant. Electron **54**, 810 (2022). https://doi.org/10.1007/s11082-022-04170-0

Aydin, F., Sari, H., Kasapoglu, E., et al.: The anisotropy effects on the shallow-donor impurity states and optical transitions in quantum dots. Eur. Phys. J. Plus **136**, 832 (2021). https://doi.org/10.1140/epjp/s13360-021-01833-x

Belaid, W., El Ghazi, H., Basyooni, M.A., et al.: Ground and two low-lying excited states binding energy in (Al, Ga)N/AlN double quantum wells: temperature and electric field effects. Philos. Mag. **102**(19), 1989–2001 (2022). https://doi.org/10.1080/14786435.2022.2100939

Bellessa, J., Voliotis, V., Grousson, R., et al.: Quantum-size effects on radiative lifetimes and relaxation of excitons in semiconductor nanostructures. Phys. Rev. B **58**(15), 9933–9940 (1998). https://doi.org/10.1103/PhysRevB.58.9933

Berrada, K., Aldaghri, O.: Coherence and entropy squeezing in the spin-boson model under non-markovian environment. Opt. Quant. Electron. **51**, 61 (2019). https://doi.org/10.1007/s11082-019-1767-2

Carles, R., Moulay, E.: Hiher order Schrodinger equations. J. Phys. A Math. Theor. 45(39): 395,304. (2012) https://doi.org/10.1088/1751-8113/45/39/395304

Chang, C.: Studies on the third-harmonic generations in a quantum ring with magnetic field. Eur. Phys. J. Plus **138**, 116 (2023). https://doi.org/10.1140/epjp/s13360-023-03733-8

Chang, C., Li, X., Wang, X., et al.: Nonlinear optical properties in gaas/ga0.7al0.3as spherical quantum dots with like-deng-fan-eckart potential. Phys. Lett. A **467**, 128–732 (2023). https://doi.org/10.1016/j.physleta.2023.128732

Chiribella, G., Kristjánsson, H.: Quantum shannon theory with superpositions of trajectories. Proc. R Soc. A **475**, 20180–903 (2019). https://doi.org/10.1098/rspa.2018.0903

Chrafih, Y., Moudou, L., Rahmani, K., et al.: Gaas quantum well in the non-parabolic case: the effect of hydrostatic pressure on the intersubband absorption coefficient and the refractive index. Eur. Phys. J. Appl. Phys. **86**, 20–101 (2019). https://doi.org/10.1051/epjap/2019190035

Citrin, D.: Excitonic spontaneous emission in semiconductor quantum wires. IEEE J. Quant. Electron **29**(6), 2117–2122 (1993). https://doi.org/10.1109/3.234477

da Silva, S.L.E.F., Corso, G.: Microseismic event detection in noisy environments with instantaneous spectral shannon entropy. Phys. Rev. E **106**, 014–133 (2022). https://doi.org/10.1103/PhysRevE.106.014133

Edet, C.O., Ikot, A.N.: Shannon information entropy in the presence of magnetic and aharanov-bohm (ab) fields. Eur. Phys. J. Plus **136**, 432 (2021). https://doi.org/10.1140/epjp/s13360-021-01438-4

Einstein, A.: Ist die trägheit eines körpers von sienem energiegehalt abhänging? Ann. Phys. Berlin **18**, 639 (1905)

En-nadir, R., El Ghazi, H., Belaid, W., et al.: Intraconduction band-related optical absorption in coupled (In, Ga)N/GaN double parabolic quantum wells under temperature, coupling and composition effects. Results Opt. **5**, 100–154 (2021). https://doi.org/10.1016/j.rio.2021.100154

Feng, L.Q., Qiu, W., Ma, X.J., et al.: Magnetic field efect on the coherence time of asymmetric gaussian confnement potential quantum well qubits. J. Low Temp. Phys. **206**, 191–198 (2022). https://doi.org/10.1007/s10909-021-02651-2

Ghetmiri, S.A., Zhou, Y., Margetis, J., et al: Study of a SiGeSn/GeSn/SiGeSn structure toward direct bandgap type-I quantum well for all group-IV optoelectronics. Opt. Lett. 42:387–390 (2017). https://opg.optica.org/ol/abstract.cfm?URI=ol-42-3-387

Golan, A., Maasoumi, E.: Information theoretic and entropy methods: an overview. Economet. Rev. **27**, 317–328 (2008). https://doi.org/10.1080/07474930801959685

Han, Q., Chen, Z., Lu, Z.: Quantum entropy in terms of local quantum bernoulli noises and related properties. Commun. Statist. Theory Methods **51**(12), 4210–4220 (2022). https://doi.org/10.1080/03610926.2020.1812654

Henning, P., Sidikejiang, S., Horenburg, P., et al.: Unity quantum efficiency in iii-nitride quantum wells at low temperature: experimental verification by time-resolved photoluminescence. Appl. Phys. Lett. **119**, 011–106 (2021). https://doi.org/10.1063/5.0055368

Iqraoun, E., Sali, A., El-Bakkari, K., et al.: Simultaneous effects of temperature, pressure, polaronic mass, and conduction band non-parabolicity on a single dopant in conical $GaAs - Al_xGa_{1-x}As$ quantum dots. Phys. Scr. **96**, 065–808 (2021). https://doi.org/10.1088/1402-4896/abf450

Khordad, R., Sedehi, H.R.R.: Comparison of bound magneto-polaron in circular, elliptical, and triangular quantum dot qubit. Opt. Quant. Electron **52**, 428 (2020). https://doi.org/10.1007/s11082-020-02531-1

Knez, I., Du, R.R., Sullivan, G.: Evidence for helical edge modes in inverted InAs/GaSb quantum wells. Phys. Rev. Lett. **107**(136), 603 (2011). https://doi.org/10.1103/PhysRevLett.107.136603

Li, P., Chen, S., Dai, H., et al.: Recent advances in focused ion beam nanofabrication for nanostructures and devices: fundamentals and applications. Nanoscale **13**(3), 1529–1565 (2021). https://doi.org/10.1039/d0nr07539f

Li, Y.: Derivation and development of noise channel information transmission capacity. Adv. Intell. Syst. Res. **147**, 560–564 (2018). https://doi.org/10.2991/ncce-18.2018.89

Liang, X., Dong, R., Ho, J.C.: Self-assembly of colloidal spheres toward fabrication of hierarchical and periodic nanostructures for technological applications. Adv. Mater. Technol. **4**(1800), 541 (2019). https://doi.org/10.1002/admt.201800541

Marko, I.P., Broderick, C.A., Jin, S., et al.: Optical gain in GaAsBi/GaAs quantum well diode lasers. Sci. Rep. **6**(28), 863 (2016)

McJunkin, T., Harpt, B., Feng, Y., et al.: Sige quantum wells with oscillating ge concentrations for quantum dot qubits. Nat. Commun. **13**, 7777 (2022). https://doi.org/10.1038/s41467-022-35510-z

Nagaraj, N., Balasubramanian, K.: Dynamical complexity of short and noisy time series. Eur. Phys. J. Spec. Top. **226**, 2191–2204 (2017). https://doi.org/10.1140/epjst/e2016-60397-x

Pan, C.C., Tanaka, S., Feezell, W., et al.: High-power, low-efficiency-droop semipolar (2021) single-quantum-well blue light-emitting diodes. Appl. Phys. Express **5**(062), 103 (2012). https://doi.org/10.1143/APEX.5.062103

Pathakoti, K., Manubolu, M., Hwang, H.M.: Nanostructures: current uses and future applications in food science. J. Food Drug Anal. **25**, 245–253 (2017). https://doi.org/10.1016/j.jfda.2017.02.004

Reddy, A.L.M., Gowda, S.R., Shaijumon, M.M., et al.: Hybrid nanostructures for energy storage applications. Adv. Mater. **24**, 5045–5064 (2012). https://doi.org/10.1002/adma.201104502

Renk, K.F.: Basics of Laser Physics For Students of Science and Engineering, pp. 1–10. Lodon, Springer Science and Business Media (2012)

Sammak, A., Sabbagh, D., Hendrickx, N.W., et al.: Shallow and undoped germanium quantum wells: a playground for spin and hybrid quantum technology. Adv. Funct. Mater. **29**(1807), 613 (2019). https://doi.org/10.1002/adfm.201807613

Scully, M.O., Zubairy, M.S.: Quantum Optics. Cambridge University Press (1997)

Shi, Y.J., Sun, G.H., Jing, J., et al.: Shannon and fisher entropy measures for a parity-restricted harmonic oscillator. Laser. Phys. **27**(125), 201 (2017). https://doi.org/10.1088/1555-6611/aa8bbf

Tshipa, M.: Second and third harmonic generation in linear, concave and convex conical gaas quantum dots. Superlatt. Microst **159**(107), 031 (2021)

Vakkuri, A., Yli-Hankala, A., Talja, P., et al.: Time-frequency balanced spectral entropy as a measure of anesthetic drug effect in central nervous system during sevoflurane, propofol, and thiopental anesthesia. Acta Anaesthes. Scand **48**(2), 145–153 (2004). https://doi.org/10.1111/j.0001-5172.2004.00323.x

Wang, S., Scarabelli, D., Du, L., et al.: Observation of dirac bands in artificial graphene in small-period nanopatterned GaAs quantum wells. Nat. Nanotechnol. **13**, 29–33 (2018). https://doi.org/10.1038/s41565-017-0006-x

Wu, N., Du, W., Hu, Q., et al.: Recent development in fabrication of Co nanostructures and their carbon nanocomposites for electromagnetic wave absorption. Eng. Sci. 13: 11–23 (2021). https://doi.org/10.30919/es8d1149

Xia, Y., Yang, P., Sun, Y., et al: One-dimensional nanostructures: synthesis, characterization, and applications. Adv Mater 15(5):353–389 (2003). https://onlinelibrary.wiley.com/doi/10.1002/adma.200390087

Xiao, W., Qi, B., Xiao, J.L.: Impurity effect of asymmetric gaussian potential quantum well qubit. J. Low Temp. Phys. **179**, 166–174 (2015). https://doi.org/10.1007/s10909-015-1276-z

Zhang, C., Wang, Z., Liu, Y., et al.: Polaron effects on the optical refractive index changes in asymmetrical quantum wells. Phys. Lett. A **375**(3), 484–487 (2011). https://doi.org/10.1016/j.physleta.2010.11.020

Zhang, C., Min, C., Zhao, B.: Optical absorption coefficients in asymmetric quantum well. Phys. Lett. A **383**(34), 125–983 (2019). https://doi.org/10.1016/j.physleta.2019.125983